A set of molecular models for alkali and halide ions in aqueous solution

Stephan Deublein,[1] Jadran Vrabec,[2] and Hans Hasse[3]

[1)] *Laboratory of Engineering Thermodynamics, University of Kaiserslautern, 67653 Kaiserslautern, Germany*

[2)] *Thermodynamics and Energy Technology, University of Paderborn, 33098 Paderborn, Germany*

[3)] *Laboratory of Engineering Thermodynamics, University of Kaiserslautern, 67653 Kaiserslautern, Germany*[a)]

This work presents new molecular models for alkali and halide ions in aqueous solution. The force fields were parameterized with respect to the reduced liquid solution density at 293.15 K and 1 bar, considering all possible ion combinations simultaneously. The experimental target data are reproduced with a high accuracy over a wide range of salinity. The ion models predict structural properties of electrolyte solutions well, such as pair correlation functions and hydration numbers. The force fields provide good predictions of the properties studied here in combination with different models for water.

Keywords: molecular modeling, force fields, electrolytes, alkali ions, halide ions

[a)] Electronic mail: hans.hasse@mv.uni-kl.de

I. INTRODUCTION

Aqueous electrolyte solutions play an important role in many industrial applications and processes in nature. Upon addition of electrolytes to solvents, the thermodynamic properties of solutions change drastically, being dominated by the strong electrostatic interactions between the ions and the solvent molecules. The influence on the properties varies with the nature of the ion species and the composition of solution[1]. Molecular simulations of electrolyte solutions allow for detailed insights into the properties of electrolyte solutions and the changes to the solvent and to other solutes due to ions. Such simulations are widely used, e.g. for studies on the influence of electrolytes on the conformation of proteins[2,3] or polymers[4,5].

The quality of molecular simulations is determined by the employed force fields. Aqueous solutions containing electrolytes were modeled by various groups since the 1970s[6]. Ever since, the ions were mainly described by one Lennard-Jones (LJ) sphere with a superimposed point charge in its center. Over time, numerous ion models[7–13] were developed. They differ in their parameters by orders of magnitude[14], depending on solvent model, ion combination and long range correction type. Peng et al.[14] were the first to analyze different models for alkali and halide ions in aqueous solution, using the consistent force field (CFF)[15] for water. The result of their study was a set of molecular models for ions that reproduces several solid state properties and the solvent structure of the liquid phase with a high accuracy.

With increasing computing power and more advanced simulation techniques, the molecular representations of ion solutions became more reliable and thereby the accuracy of the force fields became better[16–18]. Wheeler and Newman[19] focused on two distinct salts, sodium chloride and potassium chloride, in water. Their ion models were parameterized to reproduce the diffusivity of the ions in aqueous solution. The resulting parameter set[19] captures the solution density for both saline solutions in good agreement with experimental data. Weerasinghe and Smith developed molecular models for sodium chloride[20] and guanidinium chloride[21] in aqueous solution on the basis of three experimental properties: ionic radii, crystal lattice dimensions and ion-water contact distance. The resulting force fields were analyzed using the Kirkwood-Buff theory[22] and yielded a very good agreement with experimental data for aqueous solutions of these two salts. Both studies were conducted on the basis of molecular dynamics (MD) simulations for varying salinity. This parameterization

method was very recently extended to all possible alkali-chloride combinations[23] and to all combinations of alkali chloride and sodium halide salts[24]. In that study, the force fields of Na^+ and Cl^- were taken from previous work[20] and held constant, while the LJ parameters of all remaining alkali cations and all halide anions were adjusted to the three properties mentioned above[20]. The resulting ion models show a good agreement with properties they were parameterized for, i.e. for nine of 20 possible ion combinations. For the remaining 11 combinations of alkali halide salts, the authors claim an equally good agreement with experimental data. Furthermore, they claim that the results do not depend on the water model[24]. The ion models were developed using the combining rules of Good and Hope[25] and introduced one additional binary parameter for each cation to scale the cation-water interaction. In another study, Joung and Cheatham[26] developed molecular models for alkali and halide ions based on free energies of hydration, gas phase properties, radial distribution functions and crystal lattice parameters. They derived water model dependent parameter sets for the ions which showed only moderate success in the prediction of thermodynamic properties[26]. Horinek et al.[27] derived force fields for alkali and halide ions from thermodynamic solvation properties. That study resulted in one unique parameter set for the anions, while for the cations, three parameter sets were proposed that describe the energy of solvation equally well, but differ significantly in their LJ parameters. The ability of these ion models to reproduce other thermodynamic data still needs to be investigated[27].

In this paper, a set of molecular models for all alkali and halide ions in aqueous solution is presented. The models were parameterized to reproduce experimental data on the reduced liquid solution density for all ion combinations. This property as well as structural properties are reproduced over a wide range of salinity with a high accuracy. The models were developed without introducing any binary parameter that would scale the interactions of the two components individually[28]. In Section II, the methodology of the force field parameterization is explained. In Section III, the studied structural properties are introduced, while in Section IV, the results are presented. Section V concludes the work.

II. FORCE FIELD DEVELOPMENT

All simulations of this study were performed at a temperature of 293.15 K and a pressure of 1 bar. The force field type employed was the standard LJ 12-6 potential plus one coulombic

point charge

$$u_{ij} = 4\varepsilon_{ij}\left(\left(\frac{\sigma_{ij}}{r_{ij}}\right)^{12} - \left(\frac{\sigma_{ij}}{r_{ij}}\right)^{6}\right) + \sum_{l=1}^{N_{\mathrm{C},i}}\sum_{m=1}^{N_{\mathrm{C},j}} \frac{q_l q_m}{4\pi\epsilon_0 r_{lm}} \ , \tag{1}$$

where u_{ij} is the potential energy between the particles i and j with a distance r_{ij} between their LJ sites. σ_{ij} and ε_{ij} are the LJ parameters for size and energy, respectively, q_l and q_m are the charges of the solute or the solvent particles that are at a distance r_{lm}, and ϵ_0 is the vacuum permittivity. The indices l and m count the point charges, while the total number of charges of particle i is denoted by $N_{\mathrm{C},i}$. Note that Eq. (1) is given in a form that includes the interactions with water. Throughout the present simulations, the Lorentz-Berthelot combining rules[29,30] were applied for the unlike LJ interactions. No binary parameters were considered that would describe deviations from these rules[28]. Further details of the employed simulation methods are given in the Appendix.

The solvent water was predominantly modeled by the rigid, non-polarizable force field SPC/E[31], which consists of one LJ sphere and three point charges. This model is widely used for molecular simulations of biomolecules, often in combination with the GROMOS force field[32]. The SPC/E model yields a good liquid density of water at a temperature of 293.15 K. Its accuracy under these conditions is better than that of the two other widely used models for water, namely SPC[33] and TIP4P[34]. These are nonetheless often employed in conjunction with large force field libraries for biomolecules, e.g. GROMOS96[32] and OPLS-AA[35]. Over a wider temperature range, however, none the discussed water models accurately describes the liquid density of pure water, cf. FIG. 1[36].

The ions were modeled by one LJ sphere and one point charge of magnitude of +1 e for cations and −1 e for anions, respectively, located in the center of mass. Their LJ size parameter σ was adjusted to reproduce the reduced liquid solution density $\widetilde{\rho}$ over a wide range of salinity. Here, $\widetilde{\rho}$ is defined by the density of the electrolyte solution ρ and the density of the pure solvent water ρ_0 at the same temperature

$$\widetilde{\rho} = \frac{\rho}{\rho_{\mathrm{O}}} \ . \tag{2}$$

This reference was chosen, since in molecular simulation, force fields have to reproduce at least basic properties like the density accurately in order to be used for predicting more complex thermodynamic properties of the pure component itself or, in the case of electrolytes, of the mixtures[37]. Throughout the present work, the studied conditions were always $T = 293.15$ K and $p = 1$ bar. For the present parameterization, the dependence of

$\widetilde{\rho}$ on salinity x was approximated by a first order Taylor expansion around the pure water state point ($x = 0$)

$$\widetilde{\rho}(x) = \widetilde{\rho}(x=0) + \left.\frac{\mathrm{d}\widetilde{\rho}}{\mathrm{d}x}\right|_{x=0} x + O^2 = 1 + mx + O^2 \ . \tag{3}$$

The short notation m stands for the derivative of $\widetilde{\rho}$ with respect to the salinity x in the state of infinite dilution and O^2 contains all higher order terms of the expansion. The quantity m is well accessible from experimental solution density data by simple derivation. With the definition of the salinity x as the overall mass fraction of salt in aqueous solutions, the increase of $\widetilde{\rho}$ with x is almost linear for most salts considered in this study, i.e., the first order Taylor expansion according to Eq. (3) is a good approximation. The mass fraction was used in the present work to specify the salinity rather than other common measures, like molality or ion strength, because approximation (3) turns out to be particularly good when the mass fraction is used.

Using the reduced liquid solution density as the target reference is advantageous for the parameterization of ion force fields. Changes of $\widetilde{\rho}$ are due to the addition of salt and hence, on molecular level, due to the interactions between the solvent and the ions. Furthermore, the influence of deviations of the solution density ρ due to the water force field is suppressed. The present ion models were adjusted to a property that is dominated by the influence that the ions have on solution. Hence, they capture the physical behavior of the ions in solution independent on the force field employed for the solvent, i.e. they can be combined with other water models like SPC[33], TIP3P[34], TIP4P[34] and TIP4P-Ew[38] and reproduce the reduced liquid solution density as well as structural properties, cf. Section 4.

For the ion parameterization, the derivative m of the reduced liquid solution density $\widetilde{\rho}$ was systematically calculated for various cation and anion parameter sets. The LJ size parameter for the cation σ_c was varied between 1.5 and 4.5 Å and for the anion σ_a between 2.0 and 4.5 Å, with a spacing of 0.5 Å in both cases. Throughout the study, the LJ energy parameter of both ions was held constant at a value of $\varepsilon/k_\mathrm{B} = 100$ K, which is in the range of recently published data for ion LJ energy parameters that reproduce thermodynamic properties with a decent agreement[20,39]. It is important to note that the LJ energy parameter has only a minor influence on the reduced liquid solution density and hence m, cf. Section 4. The derivative m was calculated for 42 LJ size parameter combinations by molecular simulation and subsequently regressed with a polynomial function $f : (\sigma_\mathrm{c}, \sigma_\mathrm{a}) \rightarrow m$. While the de-

pendence on the cation LJ size parameter was fitted with a fourth order polynomial, the dependence of m on the anion LJ size parameter was found to be linear. The simulation results for the 42 systems as well as the regression functions are shown in FIG. 2.
The parameter set for the ions was determined by solving the optimization problem

$$f(\sigma_{\mathrm{c}}, \sigma_{\mathrm{a}}) - m^{\mathrm{exp}} = \min \ , \tag{4}$$

for all possible combinations of alkali halide salt solutions.

III. STRUCTURAL PROPERTIES

All aqueous electrolyte solutions considered in this study were analyzed with respect to various structural properties, i.e. the radial distribution function (RDF) $g_{i-\mathrm{O}}(r)$ of water around the ion i[40], the hydration number $n_{i-\mathrm{O}}$[41] and the net charge Q_i around the ion i in solution[41]. Throughout the analyses, the position of the water molecule was represented by the position of the oxygen site O.
The radial distribution function $g_{i-\mathrm{O}}(r)$ of water around the ion i indicates the structure that the ion imposes onto the solution. This quantity is well known from the literature[40] and is thus not introduced in more detail here. The hydration number $n_{i-\mathrm{O}}$ quantifies the number of solvent molecules within a given distance around the ion i. It is defined by

$$n_{i-\mathrm{O}} = 4\pi\rho_{\mathrm{O}} \int_0^{r_{\mathrm{min}}} r^2 g_{i-\mathrm{O}}(r)\mathrm{d}r \ , \tag{5}$$

where ρ_{O} is the number density of water and r_{min} is the distance up to which the hydration number is calculated. For the calculation of the hydration number within the first shell around the ion as it was used here, the value r_{min} was chosen to be the distance of the first minimum of the RDF $g_{i-\mathrm{O}}(r)$[41].
The net charge Q_i quantifies the total charge of the solution within a distance r around the ion i with a charge q_i. It is calculated by

$$Q_i(r) = \sum_j \sum_{l=1}^{N_{\mathrm{C},j}} 4\pi q_l \rho_j \int_0^r r^2 g_{i-l}(r)\mathrm{d}r \ , \tag{6}$$

where ρ_j is the number density of component j in solution. Note that for the calculation of the net charge, all components j, i.e. ions and solvent, have to be considered. A typical

radial dependence of the net charge is shown in FIG. 3 for a sodium chloride solution. For small distances from the sodium cation, the net charge drops to large negative values due to the aggregation of negatively charged chloride anions and the orientation of negatively charged oxygen atoms of the solvent towards the cation. This effect is balanced for larger distances by the bonded, partially charged hydrogen atoms of the solvent and positively charged cations, resulting in an overall positive net charge. The cycle of negatively charged shells followed by positively charged shells continues, until this oscillation of the net charge Q_i has decayed to a constant value of $-q_i$ at some distance $r_\pm$, which defines the distance up to which the electrostatic influence of an ion in the solution is significant. Throughout this study, the net charge was considered as constant when the fluctuations of the net charge around $-q_i$ have decayed to within 10% of q_i, hence $|Q(r) + q_i| < 0.1|q_i|$.

Knowledge of the distance $r_\pm$ is important for the application of local field theory approaches for the calculation of the long range electrostatic interactions, e.g. as proposed by Rodgers and Weeks[42]. These methods determine the electrostatic interactions for an ion i explicitly up to a cut-off distance r_c and estimate the remaining contribution by a constant factor, which depends on the negative charge of the ion $-q_i$. For this correction factor to be accurate, the net charge has to have decayed to $-q_i$, implying that the cut-off radius r_c has to be chosen larger than $r_\pm$.

IV. RESULTS AND DISCUSSION

Molecular models for alkali and halide ions dissolved in aqueous solutions were developed by solving the optimization problem presented in Eq. (4) simultaneously for all possible combinations of the anions and the cations studied in the present work. The full parameter set is given in Table I. The order of the LJ size parameters of the ions is consistent with their order in the periodic table of elements $Li^+ < Na^+ < K^+ < Rb^+ < Cs^+$ and $F^- < Cl^- < Br^- < I^-$. Note that the values for lithium and sodium differ only slightly. In comparison to ion radii defined according to Pauling, the LJ size parameters for all ions are larger[43], which is in agreement with other classical molecular models for the ions in the literature[19,20,44].

A. Reduced density

The present ion models reproduce the reduced liquid density well for aqueous alkali halide electrolyte solutions. Considering all combinations of ions that are soluble in water in a significant quantity, the deviations of the simulation data from the measured values[45] are below 1%, except for RbCl and RbBr at high salinity, where the deviations are 1.5%, cf. FIGs. 4 and 5. Note that LiF was excluded in this analysis since it is only soluble in traces. All density data reported here were determined by molecular simulation runs, which were fully equilibrated, i.e. the ion association that occurs in some solutions has reached a steady state.

This good agreement is not surprising, because the ion models were parameterized to the reduced liquid solution density. However, it shows that a simultaneous fit exclusively of the LJ size parameter is sufficient to cover the density of all aqueous alkali halide solutions and that no binary parameters are needed. The LJ energy parameter does not have a significant influence on the reduced liquid solution density. This result is less intuitive since dispersion influences the density of liquids as well. However, the ion's LJ size parameters dominate the reduced liquid solution density in case of aqueous electrolyte solutions, cf. FIG. 6. Variations in the LJ size parameter of $\pm 10\%$ result in density changes of up to 5%, while changes of the LJ energy parameter by orders of magnitude can hardly be discerned. The LJ energy parameter, which was set here to an arbitrary but reasonable value, is thus free for subsequent optimizations to other properties of interest.

B. Structural properties

All possible combinations of alkali cations and halide anions in aqueous solution were investigated with respect to three basic structural properties: RDF, hydration number and net charge. The general trends are discussed for each alkali and halide ion individually in the following, while the results are summarized in Table II. Note that for each investigated ion, the locations of the first maximum and of the first minimum of the ion-water RDF were found to be practically constant, independent on counterion type and salinity, which is in good agreement with experimental and simulation data[46,47]. With respect to the net charge, a charge compensation within the boundaries of the simulation volume was desir-

able. A complete compensation was not achieved in some simulations that were carried out here. However, errors induced by this should not be important given that periodic boundary conditions were used.

1. Cations

Lithium: The RDF of lithium shows the first maximum at a distance of 2.2 Å and the first minimum at 3.0 Å, cf. FIG. 7. This result is within the range of experimental data, which are available for the first maximum for this cation and vary strongly from 1.95 to 2.25 Å[46], while the ab initio calculations determined the maximum at 2.0 Å[48]. The hydration number for lithium from simulation shows a slight decay with increasing salinity, being in the range of 5.2 to 5.5. This is also in good agreement with experimental work, which determined the number of water molecules around Li^+ to be between 4 and 5.3[46]. The influence of the anion on the hydration number is small and only visible at high salinity. The electrostatic effects of lithium are long ranged. At low salinity, charge neutrality was in most cases not reached within the boundaries of the simulation volume, which were at $r \approx 15$ Å. At higher salinity, the distance for charge compensation was determined to be 9.0 Å for large counterions and 11.8 Å for small counterions.

Sodium: The sodium cation shows a similar behavior as the lithium cation. The first maximum of the RDF was found at a distance of 2.2 Å, the first minimum at 3.0 Å. This is in agreement with experimental and ab initio data, which indicate the first maximum of the RDF at a distance of 2.1 Å[46] and 2.3 Å[49], respectively. The hydration number remains almost constant at a value of 5.2 to 5.5 water molecules around the cation, independent of counterion type and salinity. This behavior was also observed in other simulation studies[46]. The influence of the charge decays slowly with the distance. At low salinity, the net charge did not decay to a constant value within the simulation volume, except for NaI, whereas at higher salinity, the distance decays down to 9.0 Å, depending on the type of counterion.

Potassium: For the potassium cation, the first maximum and minimum of the RDF are shifted to larger distances due to its larger size, being 2.6 and 3.4 Å, respectively. This is in agreement with experimental data, which locate the average distance of water molecules within the first shell between 2.6 and 2.8 Å[46]. Ab initio data locate the maximum at a distance of 2.3 Å[49]. The hydration number for potassium shows almost no dependence on

salinity for small counterions, while for larger counterions starting with chloride, the hydration number decreases strongly with salinity, ranging from 5.3 to 6.3. This behavior has not yet been observed by experiment, where the hydration number was found to have a constant value between 5 and 7[46]. The net charge around potassium varies strongly with type of counterion. At low salinity, charge neutrality was reached within the simulation volume only for the largest counterion (I^-), whereas at higher salinity, the distance of charge neutrality varies between 9.0 and 10.4 Å.

Rubidium: The simulations for the rubidium solutions predicted the first RDF peak at a distance of 2.9 Å, which is close to the experimentally observed value of 3.1 Å[50] and is in excellent agreement with ab initio calculations[51]. The minimum was observed at 3.7 Å. The calculated hydration number for rubidium of ≈7 agrees with the experimental number 6.9[50]. The influence of salinity on the hydration number can be neglected for small counterions like F^-. For large counterions, the hydration number decays with salinity by 10%. Electrostatic neutrality was reached within 8.2 to >15 Å, depending on counterion type and salinity.

Caesium: For caesium, the first maximum of the RDF is located at 3.1 Å, which is identical with the experimental value of 3.1 Å[50] and with ab initio calculations[52]. The first minimum was observed at 3.7 Å. The hydration number is independent on salinity for solutions containing fluoride anions. Here, each caesium cation was surrounded by roughly eight water molecules. For the counterions Br^- and I^-, higher salinity tends to enhance the ion-ion pairing, which is exhibited by a large decay of the hydration number. Here, the average hydration number is 6 to 7 water molecules, which is in good agreement with experimental data[46,50]. Net charge neutrality around the caesium cation was reached between 9.1 and 9.9 Å at high salinity and between 9.9 and >15 Å at low salinity.

Note that the present models for rubidium and caesium capture the structural properties in a good agreement with experimental data. This is in contrast to recently expressed thoughts in the literature[23] that only force fields considering polarization effects are capable to predict the structural properties of such electrolyte solutions.

2. Anions

Fluoride: For the fluoride anion, the simulated RDF shows the first maximum at a distance of 2.9 Å and the first minimum at 3.6 Å. The position of the maximum is in excellent

agreement with other simulation studies, where a value of 2.86 Å was found[46], and ab initio calculations, where the first maximum was observed at 2.7 Å[53]. The distances of the extrema are independent of cation type and salinity. The hydration number remains constant for small counterions and rises for larger counterions at high salinity. The average hydration number was 6 to 7, which is within the uncertainty of previous molecular simulation studies[46]. Charge neutrality around the fluoride anion was reached within 9.1 and >15 Å.

Chloride: The simulations for the chloride anion predicted a first maximum at 3.3 Å and a first minimum at 4.1 Å. The same value for the maximum was also reported in other theoretical and experimental studies[46], ab initio calculations yielded a maximum at determined to 3.2 Å[53]. The hydration number for chloride remained constant at a value of 7 for varying cations and salinity. Only for caesium at high salinity, a decay of the hydration number to 6 was observed. However, the experimentally determined trend of an increase of chloride-chloride pairing was not predicted, which is in agreement with the model of Weerasinghe and Smith[20]. The net charge for the chloride anions strongly depends on the type of counterion. It decays fast for small cations like lithium and sodium, while it decays slowly for large cations and low salinity.

Bromide: The first maximum of the RDF around bromide was at 3.4 Å, while the first minimum was at 4.1 Å. The location of the maximum is in excellent agreement with the experimental value of 3.3 Å[46], which could also be confirmed by ab initio calculations[54]. The hydration number was found to be independent on salinity in combination with small cations, whereas it decays with salinity for larger cations starting with potassium. The values are between 7 and 8 for small counterions and 6 and 7 for large counterions, depending on salinity. These tendencies were also found experimentally[46]. Charge neutrality around the bromide anion was reached at a constant value of roughly 9 Å for small cations up to potassium, while for large counterions and low salinity, the distance of $r_{\pm}$ is significantly larger.

Iodide: Present simulations of the iodide anion are in good agreement with experimental work based on X-ray diffraction, which located the maximum at 3.65 Å[46], and ab initio calculations[55], which locate the maximum at 3.5 Å. The first extrema of the RDF were observed here at distances of 3.5 Å for the maximum and 4.1 Å for the minimum. The hydration number was independent on counterion type and salinity, except for the caesium cation, where a significant decrease of the hydration number at high salinity was observed.

Ion-ion pairing seems to be preferred under these conditions. The net charge of the anion was compensated within 6.6 and 10.0 Å, depending on counterion type and salinity.

C. Transferability

Due to their parameterization to the reduced liquid solution density $\widetilde{\rho}$, the present ion models can be combined with water models other than SPC/E[31] to reasonably well describe the properties investigated here. This transferability is shown for $\widetilde{\rho}$ of aqueous chloride solutions considering three cations of varying size (Na^+, K^+, Cs^+) and four additional water models, namely SPC[33], TIP3P[34], TIP4P[34] and TIP4P-Ew[38], cf. FIG. 8. For SPC and SPC/E, the differences for $\widetilde{\rho}$ are negligible, being around 0.1% for CsCl, 0.4% for KCl and 0.4% for NaCl. SPC and SPC/E have very similar electrostatic interaction sites, and hence, the same behavior of the reduced liquid solution density was observed. The charge distribution of the TIP3P force field resembles the one of SPC and SPC/E. Although the locations of the charges are shifted significantly, their magnitudes are in between the ones of SPC and SPC/E. Therefore, the reduced liquid solution density obtained for TIP3P only slightly deviates from that for SPC and SPC/E. The differences are between 0.4% and 0.6%. For the TIP4P model, $\widetilde{\rho}$ is overestimated in comparison to the other three models. In this case, the deviations are approximately 1% for NaCl, 0.6% for KCl and 0.2% for CsCl. This behavior is due to the fact that the TIP4P force field describes the electrostatic interactions of water with larger partial charge magnitudes than the SPC and SPC/E force fields, respectively, 0.43 e for SPC/E as opposed to 0.52 e for TIP4P. This leads to an increase in polarity of the solvent and therefore to stronger attractive forces between solvent and ion and thus macroscopically to a rise in the solution density. The influence of such effects is weakened with increasing ion size and thereby, decreasing electrostatic attraction, cf. FIG. 8. A similar behavior was observed for the TIP4P-Ew force field for water. Here, the deviations of $\widetilde{\rho}$ from experimental data are comparable to the ones of TIP4P, being only slightly smaller. This is again the result of the charge set which is very similar to TIP4P in terms of positions and magnitudes.

These results show that the present force fields can be applied with varying water models, especially for salinities that are relevant for biochemical applications. An integration of the ion models in large force field libraries is therefore possible without the need for reparame-

terization to the solvent model the libraries are based on. However, for the calculation of density sensitive data at high salinity, the use of the SPC/E water model is recommended, especially for small cations.

Due to the applicability of the ion models in any combination of alkali cation and halide anion and their high accuracy with respect to the investigated quantities, the ion force fields present an improvement in comparison to the literature. To our knowledge, only Gee et al.[24] developed consistent force fields for alkali halide salts that show no dependency on the water models and are also in good agreement with experimental density data. Their ion force fields, however, deviate slightly more from experimental data of $\widetilde{\rho}$ than reported here. Furthermore, their models were adjusted considering significantly more parameters than this study. Binary interaction parameters for the cation-solvent interaction were needed to achieve the reported accuracy.

V. CONCLUSIONS

Molecular models for alkali and halide ions in aqueous solution were developed on the basis of the classical LJ approach with one superimposed point charge. The present force fields were parameterized with respect to the reduced liquid solution density for all mutual combinations of ions. The accuracy of the models is high regarding the reference property and structural data of the electrolyte solutions over a wide range of salinity. The recently expressed need for polarizable models[23] or cation dependent mixing rules[24] for the calculation of these density data and structural properties was not confirmed.

In this study, the influence of the ions on the solution was characterized in terms of the net charge around the ions. The distances for which electroneutrality was reached ranged from 7.7 to >15.0 Å, depending on the ion type and salinity.

The developed force fields for the ions were parameterized on the basis of the SPC/E water model, but may well be used with other force fields for water for the calculation of the structural properties discussed here. This transferability was shown for three aqueous electrolyte solutions containing chloride anions for the water models SPC, TIP3P, TIP4P and TIP4P-Ew that are also often used for the simulation of biological systems. However, for density sensitive data, the combination of the present ion force fields with the SPC/E water

model is recommended.

ACKNOWLEDGMENTS

The authors gratefully acknowledge financial support for the project by BMBF "01H08013A - Innovative HPC-Methoden und Einsatz für hochskalierbare Molekulare Simulation" and computational support by the Steinbuch Centre for Computing under the grant LAMO as well as the High Performance Computing Center Stuttgart (HLRS) under the grant MMHBF. The present research was conducted under the auspices of the Boltzmann-Zuse Society of Computational Molecular Engineering (BZS).

Appendix A: Simulation details

All electrolyte solutions were simulated using the classical Monte-Carlo simulation technique. The employed code was an extended version of $ms2$[56]. The simulations were performed in the isothermal-isobaric (NpT) ensemble at 293.15 K and 1 bar. Electrostatic long range contributions were considered by Ewald summation[57] with a real space convergence parameter $\kappa = 5.6$. The ions and the solvent molecules were initially placed onto a face-centered cubic lattice in random order. A physically reasonable configuration was obtained by $5,000$ equilibration loops in the canonical ensemble, followed by $80,000$ relaxation loops in the NpT ensemble. Thermodynamic averages were obtained over $500,000$ loops. Each loop consisted of $N_{\mathrm{NDF}}/3$ translational or rotational steps, where N_{NDF} indicates the total number of mechanical degrees of freedom of the system, and one volume change move. The step size, i.e. the average displacement and the rotation were set such that 50% of the total MC moves were accepted. Note that this sampling strategy was confirmed by MD calculations, which were performed for aqueous sodium chloride solutions and yielded the same results as the MC simulations. Configurations of the system were saved every 500 loops, which were used for the calculation of the pair correlation functions via post-processing. All simulations were performed with a total number of 1000 particles, i.e. water molecules and ions. Throughout the study, the simulation uncertainty of the present simulation results are within the symbol size of the figures.

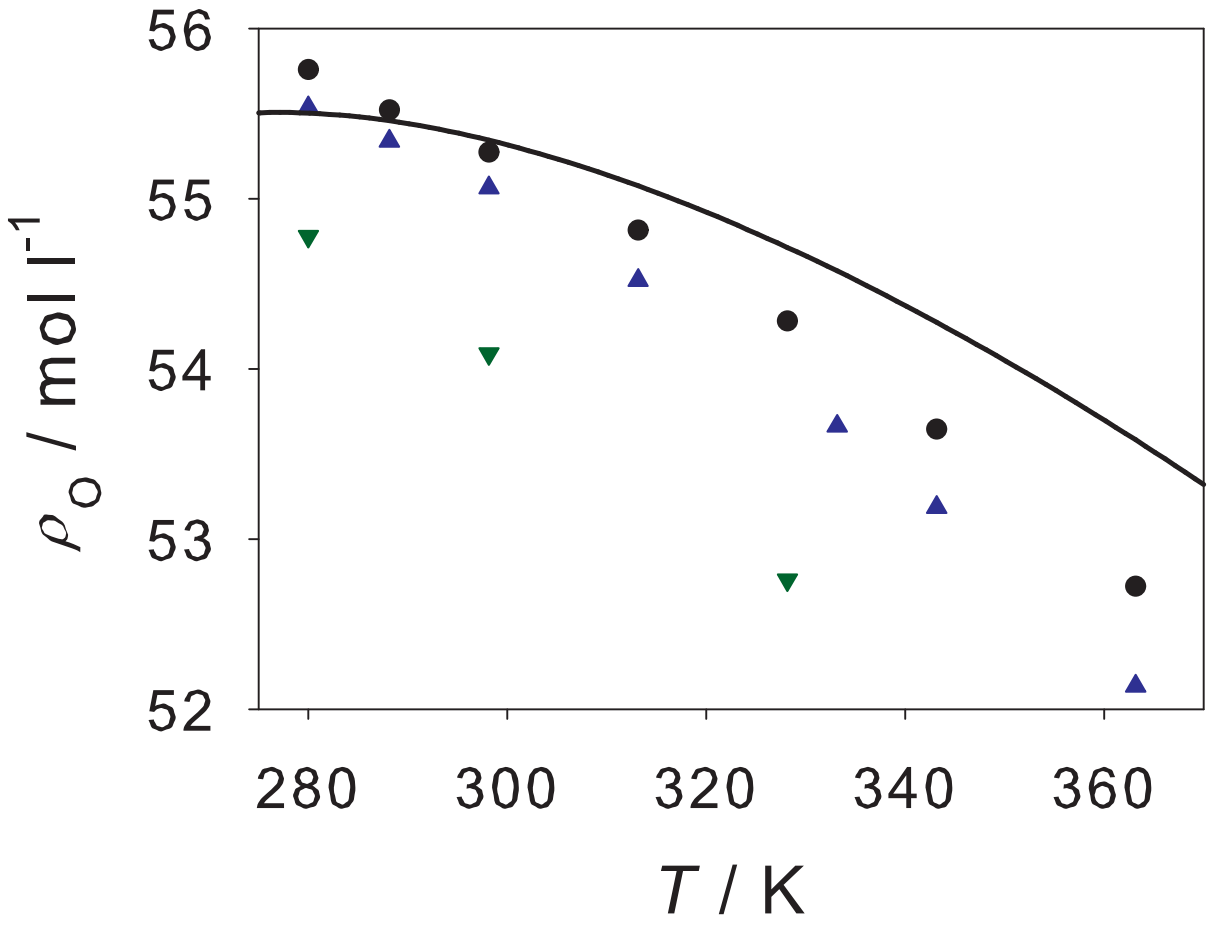

FIG. 1. Temperature dependence of the liquid density of pure water ρ_O at $p = 1$ bar. Simulation results by Guevara-Carrion et al.[36] are shown for the three water models (•) SPC/E[31], (▼) SPC[33] and (▲) TIP4P[34]. The line indicates a correlation of experimental data[58].

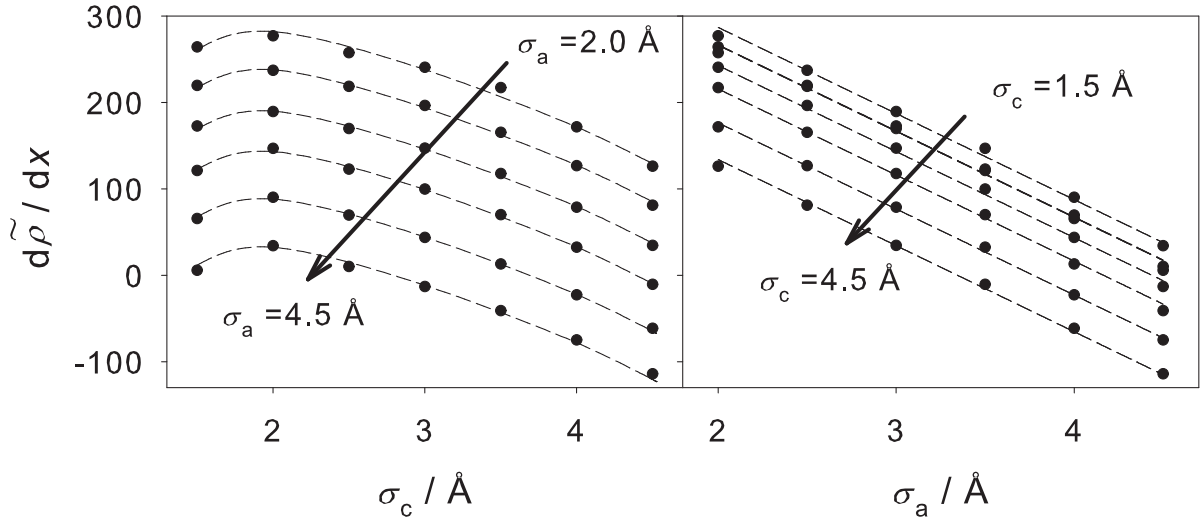

FIG. 2. Derivative of the reduced liquid solution density $\widetilde{\rho}$ with respect to salinity x. Bullets: simulation results. Dashed lines: regression using a polynomial function $f(\sigma_c, \sigma_a)$. Note that the second highest regression line in the right plot represents in fact two lines for $\sigma_c = 1.5$ and 2.5 Å.

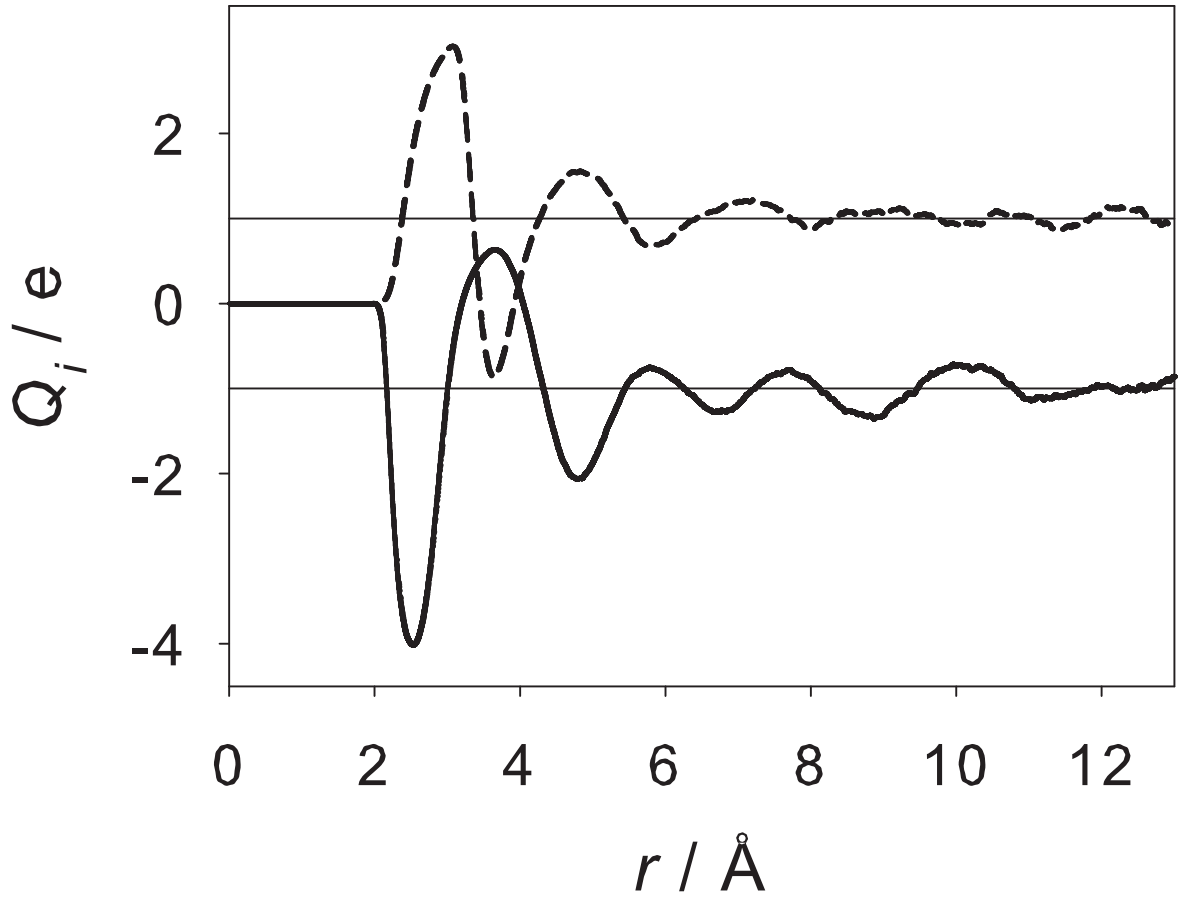

FIG. 3. Radial dependence of the net charge Q_i around the ions in an aqueous sodium chloride solution of salinity $x = 0.15$ g/g using the SPC/E model for water[31]. Solid line: Net charge around the sodium cation. Dashed line: Net charge around the chloride anion. The horizontal lines indicate charge neutralization. The influence of the ion charge decays more rapidly for the large chloride ion than for the smaller sodium ion.

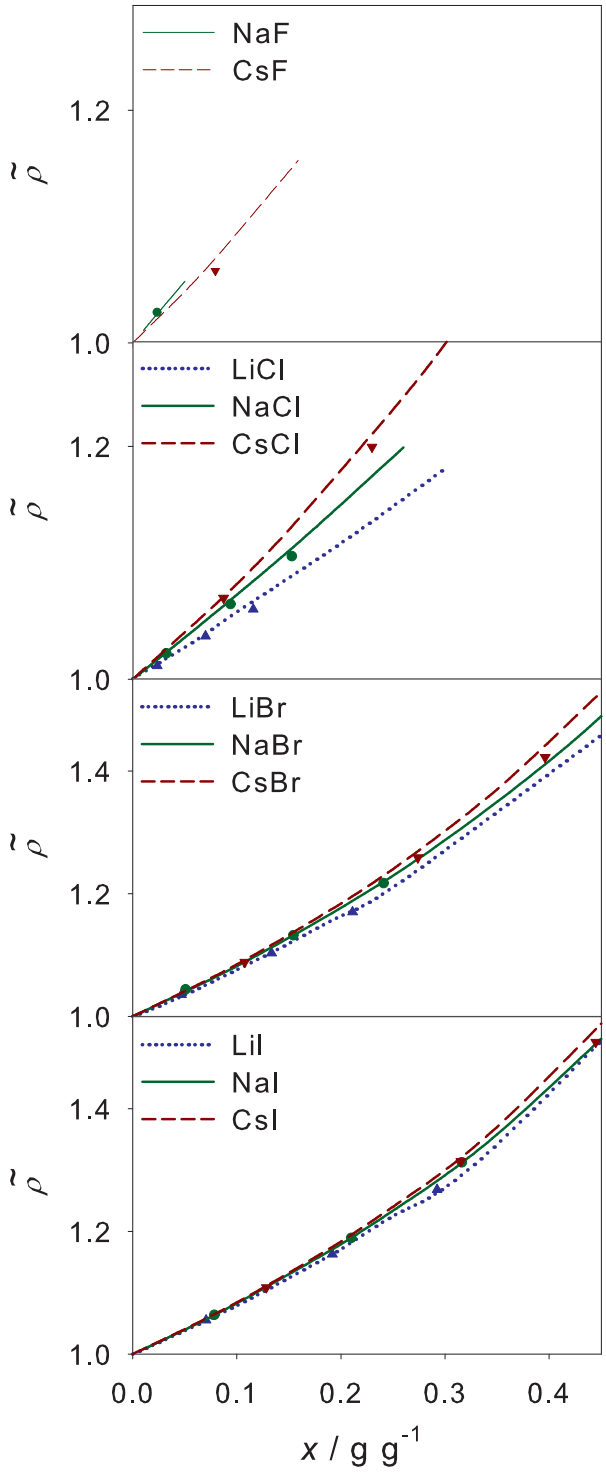

FIG. 4. Reduced liquid solution density $\widetilde{\rho}$ of aqueous electrolyte solutions for all lithium, sodium and caesium halide salts as a function of salinity x. Present simulation data (symbols) are compared to correlations of experimental data[45] (lines).

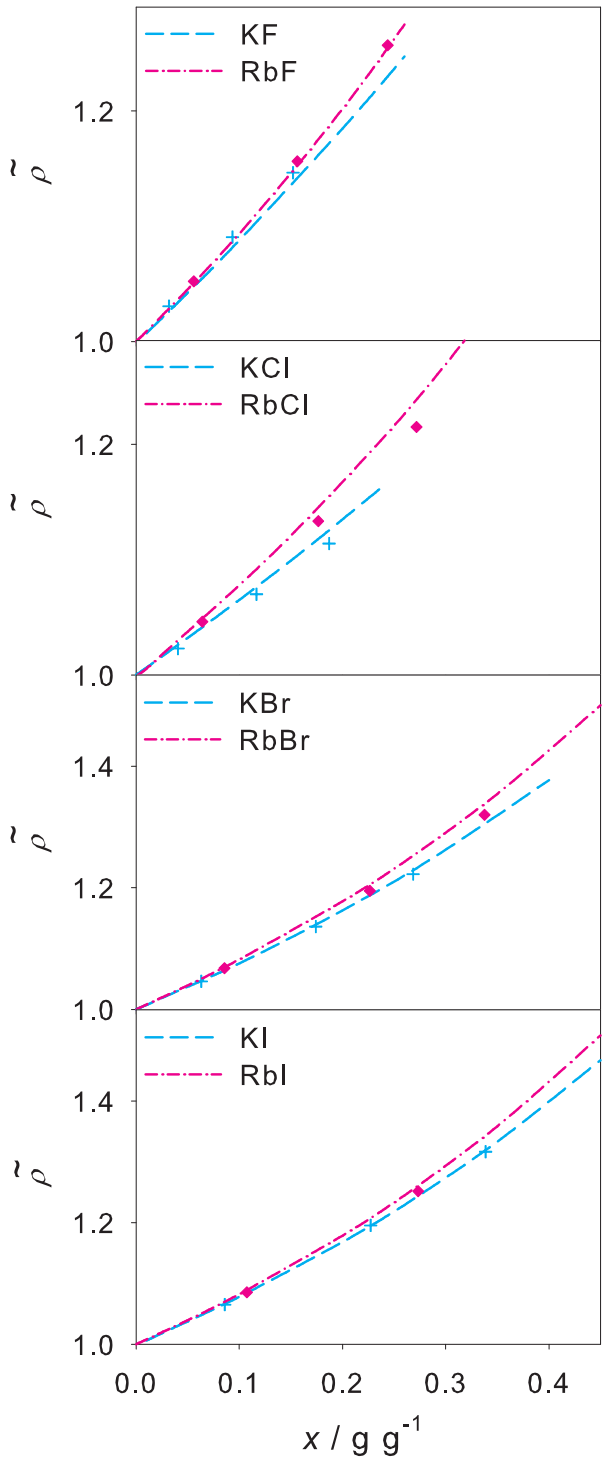

FIG. 5. Reduced liquid solution density $\widetilde{\rho}$ of aqueous electrolyte solutions for all potassium and rubidium halide salts as a function of salinity x. Present simulation data (symbols) are compared to correlations of experimental data[45] (lines).

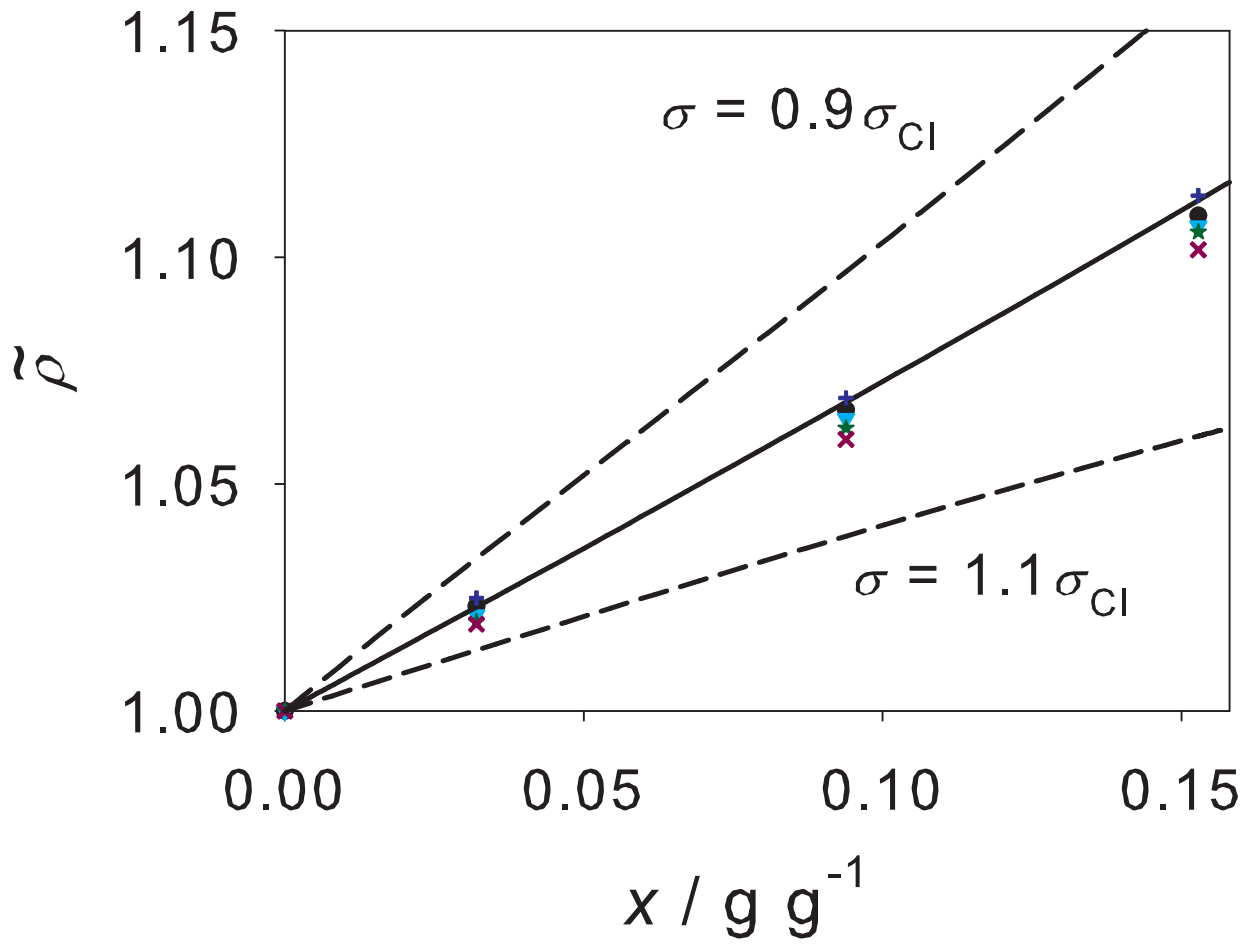

FIG. 6. Salinity dependence of the reduced liquid solution density $\tilde{\rho}$ of the aqueous sodium chloride solution. Water was described by the SPC/E model[31], while both ions were modeled by one LJ sphere with a superimposed point charge. The LJ parameters of the chloride ion were varied. Symbols: only the LJ energy parameter was varied, while the LJ size parameter remained constant $\sigma_{Cl} = 4.4$ Å: (+) $\varepsilon_{Cl}/k_B = 50$ K; (•) $\varepsilon_{Cl}/k_B = 100$ K; (▼) $\varepsilon_{Cl}/k_B = 400$ K; (⋆) $\varepsilon_{Cl}/k_B = 700$ K; (x) $\varepsilon_{Cl}/k_B = 1000$ K. Dashed lines: the LJ size parameter σ_{Cl} was varied by ±10%, while the LJ energy parameter remained constant $\varepsilon_{Cl}/k_B = 100$ K. Solid line: correlation of experimental data[45].

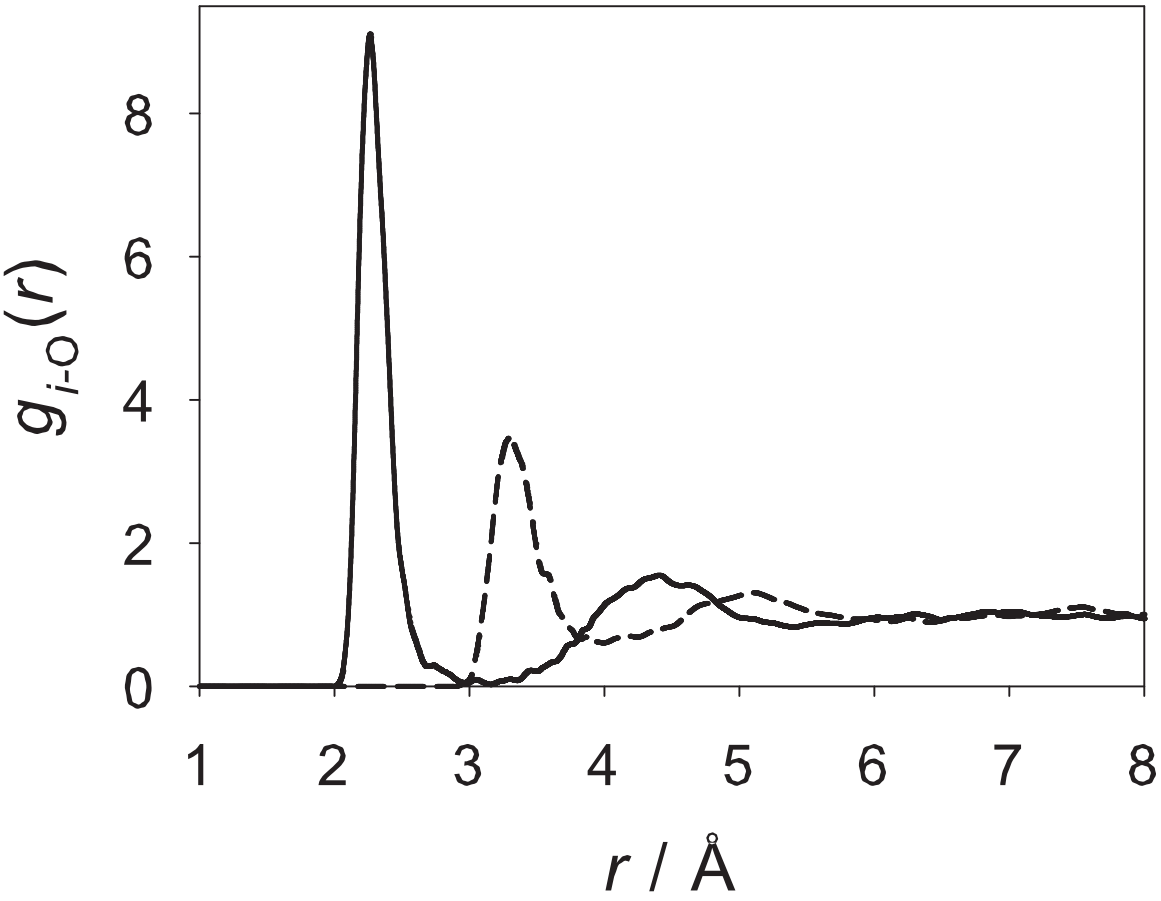

FIG. 7. Radial distribution function $g_{i-\mathrm{O}}(r)$ around Li^+ (solid line) and Cl^- (dashed line) for a salinity of $x^{(\mathrm{m})} = 0.11$ g/g. Water was described by the SPC/E model[31].

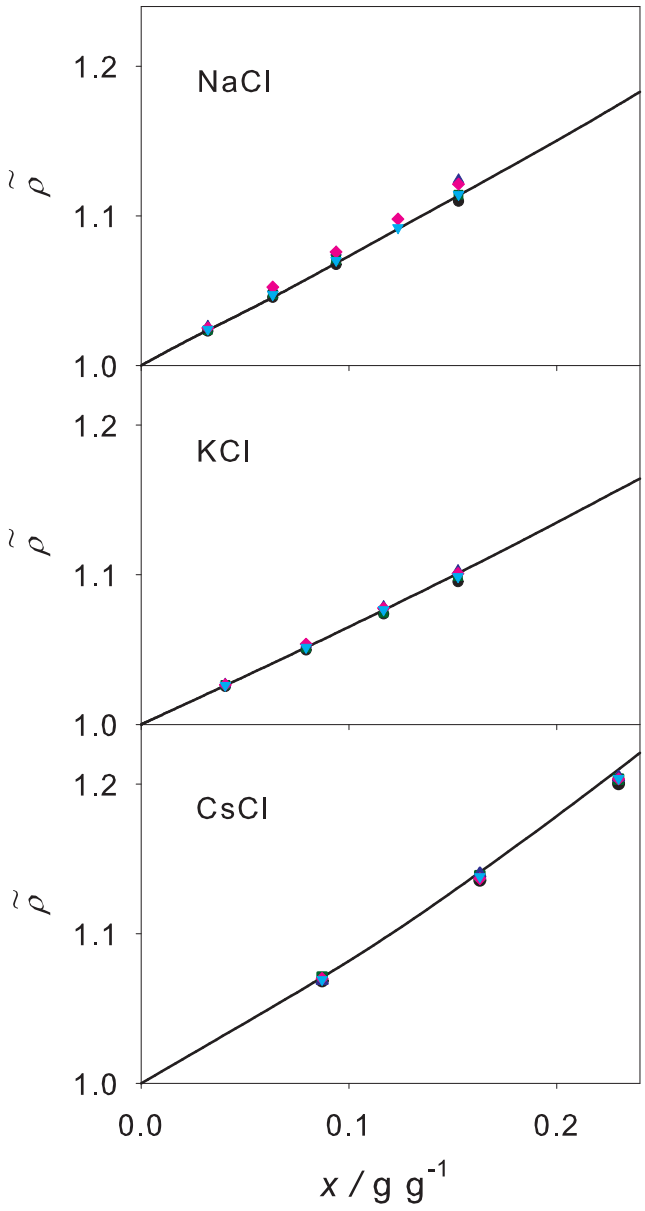

FIG. 8. Salinity dependence of the reduced liquid solution density $\widetilde{\rho}$ of aqueous XCl solutions, with X being Na^+, K^+ and Cs^+, respectively. The ions were modeled by the present force field, water was modeled by five force fields from the literature: (•) SPC/E[31], (■) SPC[33], (▼) TIP3P[34], (▲) TIP4P[34] and (♦) TIP4P-Ew[38]. The solid lines are correlations of experimental data[45].

TABLE I. LJ size parameter σ for alkali and halide ions. The LJ energy parameter is constant $\varepsilon/k_{\mathrm{B}} = 100$ K.

σ / Å								
Li^+	Na^+	K^+	Rb^+	Cs^+	F^-	Cl^-	Br^-	I^-
1.88	1.89	2.77	3.26	3.58	3.66	4.41	4.54	4.78

TABLE II: Locations of the first maximum $r_{\max}$ and the first minimum $r_{\min}$ of the ion-water RDF, hydration number $n_{i-\mathrm{O}}$ and distance of charge neutrality $r_{\pm}$. For a more compact compilation, the hydration numbers and $r_{\pm}$ are given for varying salinity in terms of the molality $x^{(\mathrm{M})}$. + denotes the cation, − the anion and O the solvent (oxygen of water). The experimental mean distance between the ion and the oxygen atom of water is: $r_{\max}^{\mathrm{Li}^+} = 2.1$ Å, $r_{\max}^{\mathrm{Na}^+} = 2.3$ Å, $r_{\max}^{\mathrm{K}^+} = 2.8$ Å, $r_{\max}^{\mathrm{Rb}^+} = 2.9$ Å, $r_{\max}^{\mathrm{Cs}^+} = 3.1$ Å, $r_{\max}^{\mathrm{F}^-} = 2.6$ Å, $r_{\max}^{\mathrm{Cl}^-} = 3.2$ Å, $r_{\max}^{\mathrm{Br}^-} = 3.4$ Å, $r_{\max}^{\mathrm{I}^-} = 3.6$ Å[46].

Salt	i	$r_{\max}$ Å	$r_{\min}$ Å	$n_{i-\mathrm{O}}$ (1 M) -	$n_{i-\mathrm{O}}$ (3 M) -	$n_{i-\mathrm{O}}$ (5 M) -	$r_{\pm}$ (1 M) Å	$r_{\pm}$ (3 M) Å	$r_{\pm}$ (5 M) Å
NaF	+	2.2	3.0	5.2	5.1	4.5	>15.0	11.4	12.1
	−	2.9	3.6	6.9	6.9	6.8	14.0	11.2	9.5
KF	+	2.6	3.4	6.4	6.2	6.0	>15.0	9.8	9.9
	−	2.9	3.6	6.8	6.7	6.3	>15.0	12.1	9.4
RbF	+	2.9	3.7	7.3	7.3	7.0	>15.0	>15.0	>15.0
	−	3.0	3.6	6.7	6.6	6.4	>15.0	12.6	11.3
CsF	+	3.1	3.8	8.0	8.2	7.6	>15.0	10.3	9.1
	−	2.9	3.6	6.8	6.5	6.5	>15.0	13.2	9.2
LiCl	+	2.2	3.0	5.5	5.4	5.2	>15.0	>15.0	11.8
	−	3.4	4.1	7.5	7.6	7.7	9.6	8.4	8.2
NaCl	+	2.2	3.0	5.6	5.4	5.3	>15.0	>15.0	11.8
	−	3.3	4.0	7.5	7.6	7.6	9.6	8.4	8.2
KCl	+	2.6	3.4	6.1	5.9	5.7	>15.0	9.9	10.4
	−	3.4	4.1	7.4	7.3	7.0	>15.0	9.9	9.4
RbCl	+	2.9	3.7	7.2	6.9	6.4	>15.0	12.6	10.0
	−	3.3	4.0	7.1	6.9	6.6	>15.0	10.1	9.8
CsCl	+	3.1	3.8	7.7	7.1	6.5	9.9	10.3	9.3
	−	3.3	4.0	7.2	6.8	6.3	>15.0	9.6	9.6
LiBr	+	2.2	3.0	5.5	5.3	5.3	>15.0	11.8	11.2
	−	3.3	4.0	7.3	7.9	7.8	9.5	9.5	9.1
NaBr	+	2.2	3.0	5.4	5.4	5.3	>15.0	11.8	11.2
	−	3.4	4.0	7.3	7.5	7.4	9.5	9.5	9.1
KBr	+	2.6	3.4	6.1	6.1	5.7	>15.0	10.0	10.4
	−	3.4	4.1	7.6	7.5	6.9	9.6	9.5	8.6
RbBr	+	2.9	3.7	7.2	6.7	6.2	>15.0	11.8	9.2
	−	3.4	4.0	7.0	6.7	6.3	12.3	9.7	8.8

Table II continued

Salt	i	$r_{\max}$ Å	$r_{\min}$ Å	$n_{i-\mathrm{O}}$ (1 M) -	$n_{i-\mathrm{O}}$ (3 M) -	$n_{i-\mathrm{O}}$ (5 M) -	$r_{\pm}$ (1 M) Å	$r_{\pm}$ (3 M) Å	$r_{\pm}$ (5 M) Å
CsBr	+	3.1	3.8	7.5	7.1	6.4	11.3	11.4	9.4
	−	3.4	4.0	7.0	6.7	6.2	13.5	9.5	8.5
LiI	+	2.2	3.0	5.4	5.3	5.4	9.0	10.8	9.0
	−	3.5	4.2	7.8	8.0	8.0	9.3	9.4	6.6
NaI	+	2.2	3.0	5.4	5.3	5.4	9.0	10.8	9.0
	−	3.5	4.2	7.8	8.0	8.0	9.6	9.6	6.6
KI	+	2.6	3.4	6.3	6.1	5.6	11.2	9.9	9.8
	−	3.5	4.2	7.6	7.7	7.5	10.1	9.7	6.6
RbI	+	2.9	3.7	6.8	6.5	6.2	11.8	11.6	8.2
	−	3.5	4.2	7.3	7.1	6.9	10.0	10.0	9.5
CsI	+	3.1	3.8	7.5	6.9	6.4	12.2	11.4	9.9
	−	3.5	4.2	7.4	7.0	6.6	10.3	9.7	9.5

REFERENCES

[1]B. Hribar, N. T. Southall, V. Vlachy, and K. A. Dill, Journal of The American Chemical Society **124**, 12302 (2002).

[2]R. L. Baldwin, Biophysical Journal **71**, 2056 (1996).

[3]Y. von Hansen, I. Kalcher, and J. Dzubiella, Journal of Physical Chemistry B **114**, 13815 (2010).

[4]Y. Zhang, S. Furyk, L. B. Sagle, Y. Cho, D. E. Bergbreiter, and P. S. Cremer, Journal of Physical Chemistry C **111**, 8916 (2007).

[5]H. B. Du, R. Wickramasinghe, and X. H. Qian, Journal of Physical Chemistry B **114**, 16594 (2010).

[6]J. C. Rasaiah, Journal of Chemical Physics **52**, 704 (1970).

[7]S. H. Lee and J. C. Rasaiah, Journal of Chemical Physics **101**, 6964 (1994).

[8]S. H. Lee and J. C. Rasaiah, Journal of Physical Chemistry **100**, 1420 (1996).

[9]S. Koneshan, J. C. Rasaiah, R. M. Lynden-Bell, and S. H. Lee, Journal of Physical Chemistry B **102**, 4193 (1998).

[10]J. Aqvist, Journal of Physical Chemistry **94**, 8021 (1990).

[11]L. X. Dang, Journal of Chemical Physics **96**, 6970 (1992).

[12]D. E. Smith and L. X. Dang, Journal of Chemical Physics **100**, 3757 (1994).

[13]L. X. Dang, Journal of the American Chemical Society **117**, 6954 (1995).

[14]Z. W. Peng, C. S. Ewig, M. J. Hwang, M. Waldman, and A. T. Hagler, Journal of Physical Chemistry A **101**, 7243 (1997).

[15]J. Fabricius, S. B. Engelsen, and K. Rasmussen, New Journal of Chemistry **19**, 1123 (1995).

[16]K. P. Jensen and W. L. Jorgensen, Journal of Chemical Theory and Computation **2**, 1499 (2006).

[17]G. Lamoureux, E. Harder, I. V. Vorobyov, B. Roux, and A. D. MacKerell, Chemical Physics Letters **418**, 245 (2006).

[18]M. M. Reif and P. H. Hunenberger, Journal of Chemical Physics **134**, 144104 (2011).

[19]D. R. Wheeler and J. Newman, Journal of Physical Chemistry B **108**, 18353 (2004).

[20]S. Weerasinghe and P. E. Smith, Journal of Chemical Physics **119**, 11342 (2003).

[21]S. Weerasinghe and P. E. Smith, Journal of Chemical Physics **121**, 2180 (2004).

[22]J. G. Kirkwood and F. P. Buff, Journal of Chemical Physics **19**, 774 (1951).

[23]B. Klasczyk and V. Knecht, Journal of Chemical Physics **132**, 024109 (2010).

[24]M. B. Gee, N. R. Cox, Y. F. Jiao, N. Bentenitis, S. Weerasinghe, and P. E. Smith, Journal of Chemical Theory and Computation **7**, 1369 (2011).

[25]R. J. Good and C. J. Hope, Journal of Chemical Physics **53**, 540 (1970).

[26]I. S. Joung and T. E. Cheatham, Journal of Physical Chemistry B **113**, 13279 (2009).

[27]D. Horinek, S. I. Mamatkulov, and R. R. Netz, Journal of Chemical Physics **130**, 124507 (2009).

[28]T. Schnabel, M. Cortada, J. Vrabec, S. Lago, and H. Hasse, Chemical Physics Letters **435**, 268 (2007).

[29]H. Lorentz, Annalen der Physik **248**, 127 (1881).

[30]D. Berthelot, Comptes Rendues de l'Academie des Sciences **126**, 1703 (1898).

[31]H. J. C. Berendsen, J. R. Grigera, and T. P. Straatsma, Journal of Physical Chemistry **91**, 6269 (1987).

[32]M. Christen, P. H. Hunenberger, D. Bakowies, R. Baron, R. Burgi, D. P. Geerke, T. N. Heinz, M. A. Kastenholz, V. Krautler, C. Oostenbrink, C. Peter, D. Trzesniak, and W. F. Van Gunsteren, Journal of Computational Chemistry **26**, 1719 (2005).

[33]H. J. C. Berendsen, J. P. M. Postma, W. F. van Gunsteren, and J. Hermans, *Intermolecular Forces*, edited by B. Pullman (D. Reidel Publishing Company, Dordrecht, 1981).

[34]W. L. Jorgensen, J. Chandrasekhar, J. D. Madura, R. W. Impey, and M. L. Klein, Journal of Chemical Physics **79**, 926 (1983).

[35]W. L. Jorgensen, D. S. Maxwell, and J. Tirado-Rives, Journal of the American Chemical Society **118**, 11225 (1996).

[36]G. Guevara-Carrion, J. Vrabec, and H. Hasse, Journal of Chemical Physics **134**, 074508 (2011).

[37]B. Eckl, J. Vrabec, and H. Hasse, Fluid Phase Equilibria **274**, 16 (2008).

[38]H. W. Horn, W. C. Swope, J. W. Pitera, J. D. Madura, T. J. Dick, G. L. Hura, and T. Head-Gordon, Journal of Chemical Physics **120**, 9665 (2004).

[39]I. S. Joung and T. E. Cheatham, Journal of Physical Chemistry B **112**, 9020 (2008).

[40]M. Allen and D. Tildesley, *Computer Simulation of Liquids* (Clarendon Press, Oxford, 1987).

[41]R. A. Robinson and R. H. Stokes, *Electrolyte Solutions*, 2nd ed. (Butterworth, London, 1955).

[42]J. M. Rodgers and J. D. Weeks, Journal of Chemical Physics **131**, 244108 (2009).

[43]E. Riedel, *Allgemeine und Anorganische Chemie*, 10th ed. (Gruyter, Berlin, 2010).

[44]P. B. Balbuena, K. P. Johnston, and P. J. Rossky, Journal of Physical Chemistry **100**, 2706 (1996).

[45]R. Weast, *Handbook of Chemistry and Physics*, 68th ed. (CRC Press, Boca Raton, 1987).

[46]Y. Marcus, Chemical Reviews **88**, 1475 (1988).

[47]S. Varma and S. B. Rempe, Biophysical Chemistry **124**, 192 (2006).

[48]H. H. Loeffler, Y. Inada, and S. Funahashi, Journal of Physical Chemistry B **110**, 5690 (2006).

[49]S. S. Azam, T. S. Hofer, B. R. Randolf, and B. M. Rode, Journal of Physical Chemistry A **113**, 1827 (2009).

[50]S. Ansell, A. C. Barnes, P. E. Mason, G. W. Neilson, and S. Ramos, Biophysical Chemistry **124**, 171 (2006).

[51]T. S. Hofer, B. R. Randolf, and B. M. Rode, Journal of Computational Chemistry **26**, 949 (2005).

[52]C. F. Schwenk, T. S. Hofer, and B. M. Rode, Journal of Physical Chemistry A **108**, 1509 (2004).

[53]A. Tongraar, S. Hannongbua, and B. M. Rode, Physical Chemistry Chemical Physics **5**, 357 (2003).

[54]S. Raugei and M. L. Klein, Journal of Chemical Physics **116**, 196 (2002).

[55]A. Tongraar, S. Hannongbua, and B. M. Rode, Journal of Physical Chemistry A **114**, 4334 (2010).

[56]S. Deublein, B. Eckl, J. Stoll, S. V. Lishchuk, G. Guevara-Carrion, C. W. Glass, T. Merker, M. Bernreuther, H. Hasse, and J. Vrabec, Computer Physics Communications **182**, 2350 (2011).

[57]P. P. Ewald, Annalen der Physik **64**, 253 (1921).

[58]W. Wagner and A. Pruss, Journal of Physical and Chemical Reference Data **31**, 387 (2002).